

UDC 666.11.0

## PERLITE-BASED NANOSTRUCTURED GLASS-CERAMIC: PREPARATION AND INVESTIGATION

S. G. Petrosyan,<sup>1,2</sup> L. N. Grigoryan,<sup>3</sup> and P. G. Petrosyan<sup>3</sup>

Translated from *Steklo i Keramika*, No. 10, pp. 39–47, October, 2023.

*Original article submitted December 27, 2022.*

Perlite, an inexpensive mineral raw material, served as a base to synthesize an opaque glass-crystalline material containing in the bulk nanosized wollastonite and gehlenite crystals of average size 100 nm. The phase composition, microstructure, and strength properties of the material were investigated. Changes effected in the composition and size of the crystal grains by varying the amount of catalyst and silica content in the initial mixtures make it possible to control the physical and mechanical properties of the resulting material. High strength and high hardness make it possible to use this material for protection against high-velocity impacts, including bullets from firearms.

**Keywords:** glass-ceramic, perlite, nanocrystals.

### INTRODUCTION

Substantial progress has been made in the development of new glass-ceramic (glass-crystalline) materials with unique physicochemical and chemical properties [1, 2]. On account of their thermal and chemically resistant properties, mechanical strength, and dielectric properties such materials are widely used as substrates for microcircuits, in heat exchangers and chemical reactors, electronic and space technology, the chemical industry, military practice, and elsewhere [3, 4].

Glass-ceramic (GC) materials are produced by catalyzed crystallization of glass of a certain composition, in which process nuclei are formed and bulk or surface crystallization of various phases occurs, so that the material transforms into a polycrystalline structure [5, 6]. Glass-ceramics, as a rule, have a fine-grained structure, the size of its crystalline grains, uniformly distributed in the residual glass matrix, is usually less than 1  $\mu\text{m}$  [7], which is many times smaller than the grain size in conventional ceramic materials. With certain compositions, it is possible to obtain GC material with an ultrafine structure, when the crystallite sizes are smaller than

100 nm. Such GC materials, called nanocrystalline [8, 9], possess a high elastic modulus and make it possible to polish their surfaces to an average roughness level of 5  $\text{\AA}$ . The main properties of GC materials (mechanical strength, ballistic efficiency, dielectric constant, chemical stability, linear thermal expansion coefficient, etc.) can be systematically controlled, since they depend not only on the chemical composition of the original glass, but also on the resulting crystalline phases, grain sizes, and residual glass/crystal phase ratios [5, 10].

Much attention also goes to special types of glass ceramics, which are simultaneously characterized by heightened mechanical strength and transparency in the optical or radio ranges of electromagnetic waves [11, 12].

A variety of natural and artificial raw materials can be used to obtain GC materials [7, 10, 13]. The main components of GC materials are usually silica  $\text{SiO}_2$ , alumina  $\text{Al}_2\text{O}_3$ , oxides of sodium  $\text{Na}_2\text{O}$ , calcium  $\text{CaO}$ , and magnesium  $\text{MgO}$  [6]. Based on the chemical composition of natural materials of volcanic origin such as perlite [14, 15], it can be argued that perlite can be used as the main raw material for the synthesis of a new type of GC material.

For example, in [16] glass-ceramic substrates for electronic devices and circuits were successfully synthesized by means of simultaneous sintering–crystallization of perlite glass powder.

The present work is devoted to the preparation and study of the physical and mechanical properties of perlitic GC-ma-

<sup>1</sup> Russian-Armenian (Slavic) University, Yerevan, Armenia (e-mail: stepan.petrosyan@rau.am).

<sup>2</sup> Institute of Radiophysics and Electronics NAS RA, Ashtarak, Armenia (e-mail: stepan.petrosyan@rau.am).

<sup>3</sup> Yerevan State University, Yerevan, Armenia (e-mail: l.grigoryan@ysu.am).

**TABLE 1.** Basic Chemical Composition of Perlite from the Aragats Deposit (Armenia)

Index	SiO <sub>2</sub>	Al <sub>2</sub> O <sub>3</sub>	CaO	MgO	Fe <sub>2</sub> O <sub>3</sub>	TiO <sub>2</sub>	Na <sub>2</sub> O + K <sub>2</sub> O
Weight content of the components, %	73.00	13.12	0.84	0.24	0.82	0.22	7.72

terial depending on the amount of silica transferred from perlite to the glass composition and on the content of the crystallization catalyst added to the initial composition of the glass. In addition, the possible control intervals will be found, depending on the composition of the initial charge, for controlling the properties of the synthesized material.

## MATERIALS AND INVESTIGATIVE METHODS

The synthesis process begins with the preparation and mixing of the starting glass components. The basic make-up of the prepared charge (wt.%) consisted of perlite from the Aragatskoe deposit in Armenia (the chemical make-up of perlite is presented in Table 1) — 30–60; CaCO<sub>3</sub> — 30–40; Na<sub>2</sub>CO<sub>3</sub> — 0–5. To create conditions for heterogeneous crystallization, a catalyst from the fluoride group is introduced in amounts 0–8 wt.% into the glass composition. Electron-microscopy shows that the choice of such a catalyst and its content in the initial glass composition and crystallization conditions are key factors for obtaining GC materials with a nanocrystalline structure

Glass melting was conducted for 8–10 h at 1350–1400°C in corundum crucibles. After melting, glass is formed and then annealed at 500–530°C. Next, to create the necessary microstructure, the samples underwent heat treatment in two stages. First, on soaking at 600–650°C for 1 h, crystalline nuclei form and grow, which creates a framework that strengthens the sample and prevents its deformation. At the second stage, the temperature is raised to 750–850°C and the sample is soaked in order to crystallize the main substance of the glass. In the course of the entire crystallization process, the rise rate of the temperature did not exceed 5 K/min. The homogeneity of the initial charge and the controllability of the crystallization process make it possible to obtain a GC-material with a fine-grained structure and high mechanical strength.

The elemental composition of the GC-material was determined by energy-dispersive x-ray spectral microanalysis using a Stereoscan-360 scanning electron microscope combined with a Link AN10000 analyzer (USA). The phase composition of the GC-material was identified using the x-ray diffraction technique using a PANalytical BV diffractometer (Holland) (CuK $\alpha$  radiation). The kinetics of crystallization was studied by non-isothermal differential thermal analysis (DTA) using a Paulik–Paulik–Erdey Q-1500D derivatograph (Hungary). The reference material was calcined Al<sub>2</sub>O<sub>3</sub> powder, sample weight 1 g. The microhardness of the GC samples was measured with a Digital MicroVickers HardnessTester DV-1At-8 (China), the microstructure of the samples was studied with a scanning electron microscope

**TABLE 2.** Starting Make-Ups for the Synthesis of Series-A GC Samples

Sample No.	Perlite, %	CaCO <sub>3</sub> , %	Na <sub>2</sub> CO <sub>3</sub> , %	Catalyst from the fluoride group, %
A1	52.0	43.0	3.0	2.0
A2	52.0	42.5	3.0	2.5
A3	52.0	42.0	3.0	3.0
A4	52.0	41.0	3.0	4.0
A5	52.0	40.0	3.0	5.0
A6	52.0	39.0	3.0	6.0
A7	52.0	38.0	3.0	7.0

(SEM) Vega-Tescan (Czech Republic), surface morphology The SC material was studied using images obtained with an atomic force microscope (AFM) SolverNext NT-MDT (St. Petersburg). The velocities of longitudinal and transverse ultrasonic waves in the GC material were determined using a pulsed Ultrasound installation (Russia). The density of the material was measured by hydrostatic weighing.

## RESULTS AND DISCUSSION

### Phase composition and microstructure

Numerous GC samples were synthesized in the above range of the make-up of the initial charge, including two series of samples with different contents of SiO<sub>2</sub> (calculated taking into account the glass transferred from perlite to the initial composition and added silica) and the crystallization catalyst. In the first series of samples (series A), the perlite content (and, accordingly, SiO<sub>2</sub>) remained constant, and the catalyst content was increased by reducing the amount of CaCO<sub>3</sub> in the initial charge (Table 2). In the synthesis of the second-series (series B) samples, the SiO<sub>2</sub> content changed, increasing on account of CaCO<sub>3</sub> content reduction (Table 3). Of note, the catalyst content remained constant at 7% in the synthesis of all samples of series B. Homogeneous and void-free GC samples were obtained as a result of crystallization.

An example of the elemental composition of one of the series-A (A7) samples of perlite glass ceramics is shown in Fig. 1. The main elements in this material were C, O, Si, Al, Ca, Na, F (at.%): 12.23, 52.47, 6.92, 3.39, 7.22, 4.16, and 2.75 respectively. Note that the same elemental composition, but in different percentages, is characteristic of all of the series-A and -B samples.

To study the kinetics of crystallization and to determine the optimal temperature ranges of crystallization, DTA of the

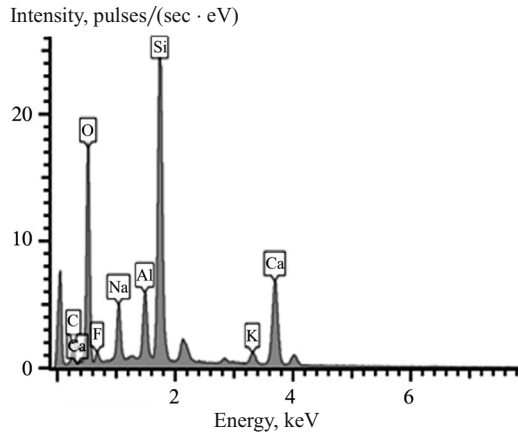


Fig. 1. Elemental make-up of an A7 sample of perlite glass-ceramic.

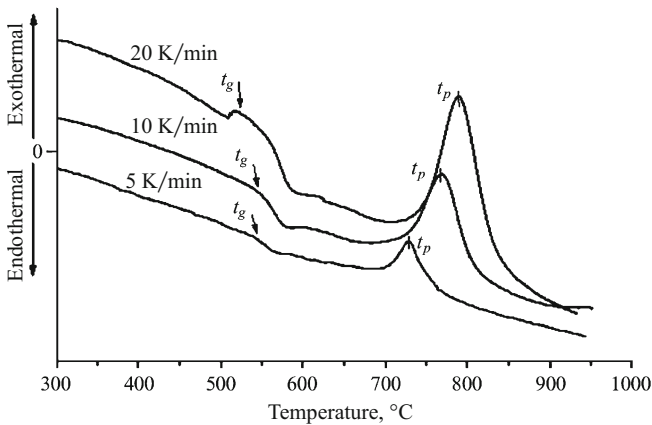


Fig. 2. DTA curves for glass-like perlite sample A7. The curves were obtained for different rates of heating.

obtained samples was conducted at different heating rates in the range 300 – 1000°C. It is clear from the curves shown in Fig. 2 that for a typical sample (A7) two thermal effects appear at all heating rates: endothermic in the glass transition temperature range (glass transition temperature  $t_g$  near

TABLE 3. Starting Make-Ups for the Synthesis of Series-B GC Samples

Sample No.	Perlite, %	CaCO <sub>3</sub> , %	Na <sub>2</sub> CO <sub>3</sub> , %	Catalyst from the fluoride group, %
B1	20	70	3	7
B2	30	60	3	7
B3	35	55	3	7
B4	40	50	3	7
B5	45	45	3	7
B6	55	35	3	7
B7	60	30	3	7
B8	65	25	3	7
B9	70	20	3	7

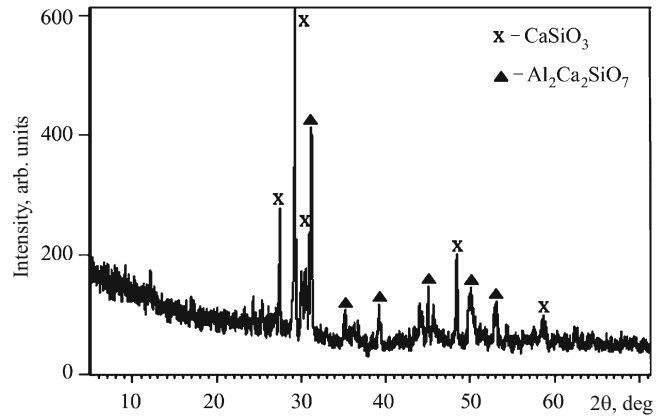


Fig. 3. X-ray diffraction pattern (CuKα) of sample A7.

550°C) and exothermic on account of glass crystallization (maximum crystallization temperature  $t_p$ ). The exothermic peak is in the range 730 – 820°C, and as the heating rate increases, the maximum crystallization temperature shifts towards higher temperatures. Of note, similar DTA curves obtain for most series-A and -B samples.

Analysis of x-ray diffraction spectra leads to the conclusion that, depending on the make-up of the initial charge and the amount of catalyst, the formation of six main crystalline phases is possible, including calcium silicates CaSiO<sub>3</sub> (wollastonite), dicalcium Ca<sub>2</sub>SiO<sub>4</sub>, tricalcium Ca<sub>3</sub>SiO<sub>5</sub> (alite), and Al<sub>2</sub>Ca<sub>2</sub>SiO<sub>7</sub> (gehlenite), Al<sub>2</sub>Ca<sub>3</sub>Si<sub>2</sub> (aluminum-calcium silicate), and Al<sub>1.66</sub>Ca<sub>0.68</sub>Na<sub>0.3</sub>Si<sub>2.34</sub>O<sub>8</sub> (labradorite).

For example, Fig. 3 shows the diffraction spectrum for a sample with catalyst of about 7%. Diffraction peaks are visible at angles  $2\theta = 27.4402^\circ, 29.2035^\circ, 30.8832^\circ, 48.358^\circ,$  and  $58.4470^\circ$ , which correspond to reflection from the crystallographic planes (–202), (023), (212), (–334), (027) of wollastonite CaSiO<sub>3</sub>. In addition to this main crystalline phase, diffraction lines are also clearly visible in this sample at the angles  $31.1905^\circ, 35.2238^\circ, 39.1596^\circ, 44.9475^\circ, 50.0883^\circ,$  and  $53.0458^\circ$ , characteristic of the crystallographic planes (121), (002), (112), (122), (041), and (331) of gehlenite Al<sub>2</sub>Ca<sub>2</sub>SiO<sub>7</sub>.

The duration of the crystallization process significantly affects the microstructure of the GC material. Figure 4 displays images of the surface of the GC material taken using SEM. No features were found in the initial glass phase. However, after heat treatment, when the sample was subjected to crystallization, at 850°C for 2 h, volumetric phase separation in the GC material clearly manifests itself, crystalline grains appear, distributed evenly in the glassy matrix. On subsequent increase in the crystallization time, an increase in the size of the crystals occurs – they grow together and combine into elongated crystals of a micrometer scale. As a result, the crystal/glass volume ratio increases.

Similar transformations of the microstructure are shown by AFM images of the polished surfaces of the GC sample (Fig. 5). It is clear from the AFM images that the average surface roughness of the nanostructured sample does not ex-

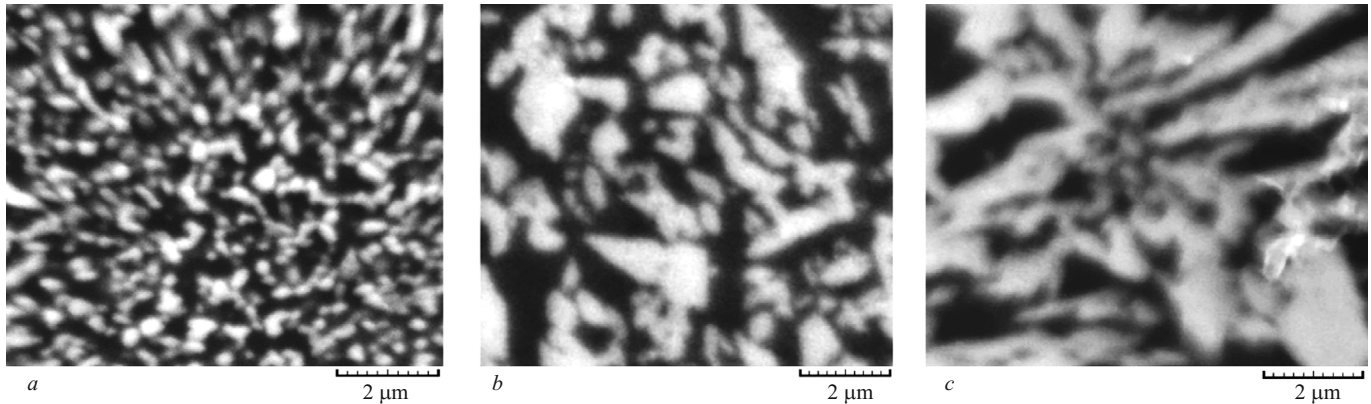


Fig. 4. Surface images of the GC material taken using SEM (sample A7), at different crystallization times: a) 2 h; b) 4 h; c) 6 h.

ceed 8 nm, which is a consequence of the fine-grained quality of the GC material

Using AFM images, the size distribution of crystalline grains was analyzed at different catalyst contents. For example, the distribution of crystals over the diameter  $d$  for sample A7 is shown in Fig. 6, showing that this distribution, similar to other nanomaterials [17], is close to log-normal and is characterized by the distribution function

$$f(d) = \frac{1}{d\sqrt{2\pi\sigma^2}} \exp\left\{-\frac{(\ln d - \ln d_0)^2}{2\sigma^2}\right\}, \quad (1)$$

where  $\sigma$  and  $d_0$  are constant parameters.

The best comparison with experimental data is obtained at  $d_0 = 113$  nm,  $\sigma = 0.59$ . Knowing these parameters, from the known dependencies [17] it is easy to estimate the average diameter  $d_{av}$  of grains and the standard deviation of the quantity  $\tilde{\sigma} = (d - d_{av})^2$ :

$$d_{av} = d_0 \exp\left(\frac{1}{2}\sigma^2\right) = 135.35 \text{ nm},$$

$$\tilde{\sigma} = d_0^2 \exp(\sigma^2)[\exp(\sigma^2) - 1] = 7917.7 \text{ nm}^2. \quad (2)$$

Note that similar studies conducted for a series of B samples show that an increase in the average grain diameter is observed as the catalyst content decreases.

### Mechanical strength of GC material

The mechanical strength of a material is one of its most important characteristics, since high strength is often the main requirement that determines the suitability of a given material for a specific practical application. The mechanical strength of the GC material, the compressive strength, and the Vickers microhardness were measured; the elastic moduli were found by the means of ultrasonic velocities.

Microhardness measurements were performed on more than 10 samples of this composition, after which their average values were taken. The spread of the results of measurements of microhardness, sound speed and density did not ex-

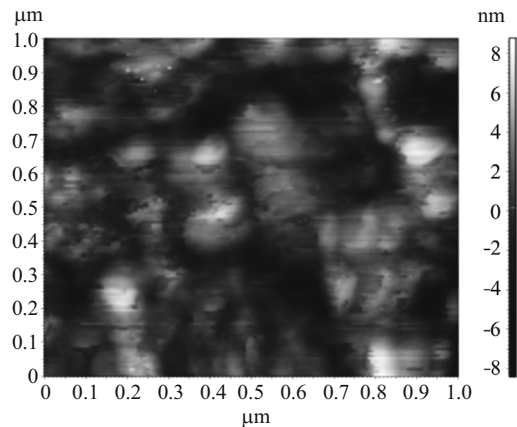
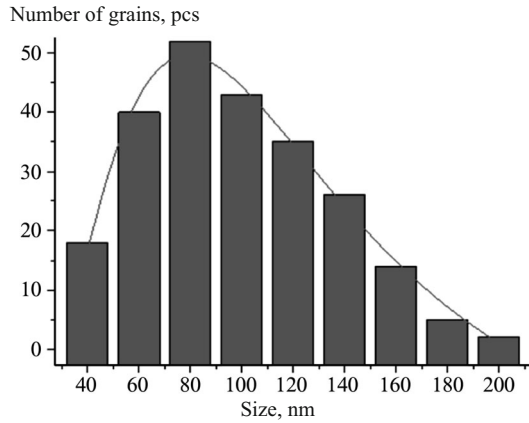


Fig. 5. Surface morphology of the GC sample A7, recorded by means of AFM.

ceed 10.0; 5.0 and 1.5%, respectively, and the measurement accuracy did not exceed 1%. To measure the tensile strength, rods with transverse dimensions of  $4 \times 5$  mm and a length of 12.5 mm were made. All measured mechanical parameters show a strong dependence on the catalyst content. As the catalyst content and the concentration of crystallization centers increase, the tensile strength increases, gradually reaches saturation and approaches a limit of about 1000 MPa. In terms of this parameter, the synthesized perlitic glass ceramic is not inferior to modern bio-ceramic such as Cerabone RA/W, containing wollastonite crystals [18].

At room temperature, perlitic glass ceramics, like normal glass or ordinary ceramics, is a brittle material, i.e. it behaves like a perfectly elastic material up to the failure load. At a lower concentration of crystallization centers, as a rule, large crystal grains are formed, which effects mechanical strength reduction of the GC material. At high catalyst concentrations, nanometer-sized crystalline grains are formed throughout the sample volume, separated by glassy layers, and the mechanical strength and hardness of the SC material, as a rule, increase. This behavior of GC material, which is characteristic of nanocrystalline materials, is often described by the Hall–Petch law and can be explained by the inhibition of



**Fig. 6.** Size distribution of grains in sample A7: solid curve) approximation using log-normal distribution (parameters  $d_0 = 113$  nm,  $\sigma = 0.59$ ).

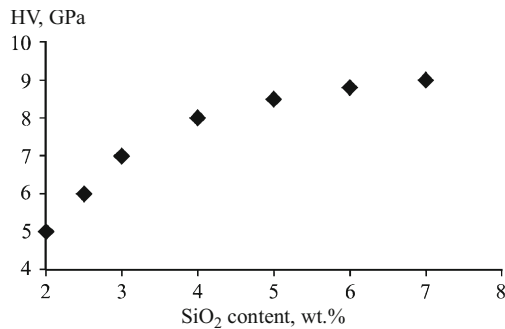


**Fig. 7.** Microhardness of samples of series-A GC material versus the catalyst content in the initial charge.

a gliding dislocation by dislocations nucleated along the grain boundary, the density of which is proportional to the surface area of the grain [19].

As follows from Fig. 7, the microhardness of the GC material increases with increasing catalyst content. For the sample A7, the catalyst content being 7 wt.%, the microhardness reaches 9 GPa. The microhardness of GC material can also be controlled by changing the SiO<sub>2</sub> content in the glass composition. It is clear from Fig. 8 that in order to obtain maximum microhardness near 8.5 GPa the initial content of perlite in the glass composition should be chosen so that the amount of SiO<sub>2</sub> in the initial mixture is equal to about 40%.

Thanks to its high hardness and relatively low density, perlite ceramic can be used for protection against high-velocity impacts, including firearm bullets. It is well known that on interacting with a solid high-speed impactor, large compressive stresses arise between the impact area and the adjacent ceramic areas these impacts are accompanied by shock waves [20]. The modular characteristics of ceramic are responsible for the resistance to fracture deformation and therefore must be as high as possible in order to curtail the damaging effect. The main physicomaterial characteristics that determine the ballistic efficiency of a material include grain size and ultrasonic speed in the material. As al-

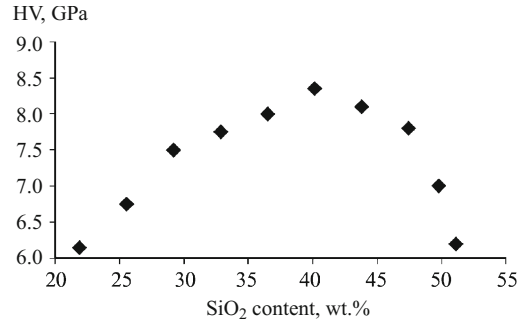


**Fig. 8.** Microhardness versus the calculated SiO<sub>2</sub> content for series-B samples.

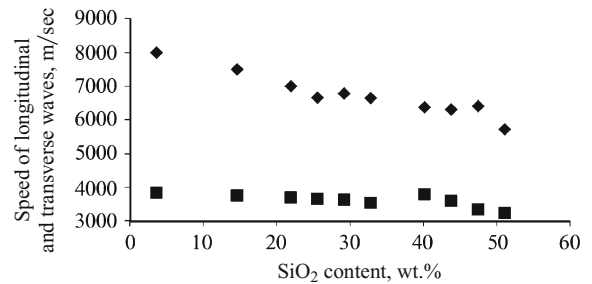


**Fig. 9.** Velocities of transverse (■) and longitudinal (◆) acoustic waves in series-B perlite GC material versus the calculated SiO<sub>2</sub> content.

ready mentioned, the grain size not only largely determines the hardness of a material but it is also an important ballistic characteristic of the GC material — the number of wave paths necessary to destroy the material under impact. As a rule, the smaller the grain size, the larger the number of wave paths [21, 22]. As for the speed of sound in a material, it determines how effectively the energy of the striking element can be dissipated away from the site of impact and depends on the Young’s modulus and density — the higher the Young’s modulus and the lower the density of the material, the higher the speed of sound in it [23, 24]. High sound speeds also indirectly indicate good compaction or low porosity of the material.

For this purpose, the dependences of the propagation speed of longitudinal and transverse ultrasonic waves in samples of perlite were determined as a function of the content of SiO<sub>2</sub> in the starting charge (Fig. 9). The density of the material was also determined by the hydrostatic weighing method (Fig. 10). It is clear from Figs. 9 and 10 that the SiO<sub>2</sub> content greatly affects the speed of transverse and longitudinal waves, as well as the density, which ultimately determines the ballistic resistance of the material.

The elastic constants of the material were calculated based on the data in Figs. 9 and 10. It turns out that for a constant concentration of crystallization centers and SiO<sub>2</sub> weight content increasing 4 to 50% in the initial charge, the Poisson ratio changes from 0.21 to 0.30, the density of the material drops by almost 20%, and the elastic and shear moduli de-

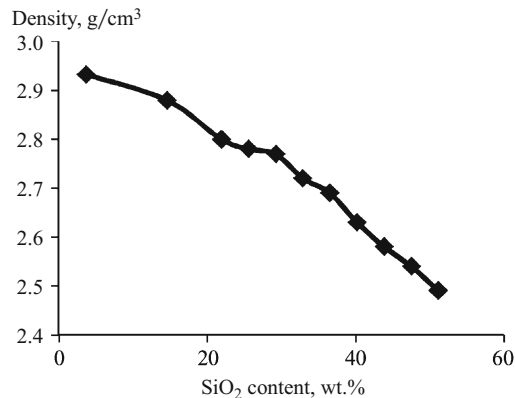


**Fig. 10.** Density of series-B samples versus the calculated SiO<sub>2</sub> content in the starting charge.

crease from 100 to 65 GPa and 40 to 25 GPa, respectively. In other words, it can be argued that the main factors controlling the mechanical strength of perlite glass ceramics are grain size and content of SiO<sub>2</sub> and catalyst.

## CONCLUSIONS

Nanostructured glass ceramic whose physical and mechanical properties hold promise for different applications was synthesized based on the perlite rock that is widespread in Armenia. The microstructure was investigated and the microhardness and elastic moduli of the resulting glass-crystalline material were determined. X-ray measurements show that the main crystalline phases are wollastonite CaSiO<sub>3</sub> and gehlenite Al<sub>2</sub>Ca<sub>2</sub>SiO<sub>7</sub>. The compressive strength and microhardness of the material are mainly determined by the average grain size, which is equal to 100 nm. High strength and hardness also make it possible to use this material to create opaque protective structures.

## REFERENCES

1. Kamakashi Narang (ed.), *Glass-Ceramics: Properties, Applications and Technology*, Nova Sci. Publ., New York (2018).
2. E. D. Zanutto, "Bright future for glass-ceramics," *Am. Ceram. Soc. Bull.*, **89**(8), 19 – 27 (2018).
3. M. J. Davis and E. D. Zanutto, "Glass-ceramics and realization of the unobtainable property combinations that push the envelope," *Mater. Res. Soc. Bull.*, **42**, 195 – 199 (2017).
4. P. D. Sarkisov, L. A. Orlova, N. V. Popovich, et al., *Vse Materialy, Entsikloped. Sprav.*, No. 8, 17 – 24 (2011).
5. J. Deubener, M. Allix, M. J. Davis, et al., "Updated definition of glass-ceramics," *J. Non-Cryst. Solids*, **501**, 3 – 10 (2018).
6. G. A. Khater, E. M. Safwat, J. Kang, et al., "Some types of glass-ceramic materials and their applications," *Intern. J. Res. Studies Sci., Eng. Technol.*, **7**(3), 1 – 16 (2020).
7. E. B. Ferreira, E. D. Zonotto L. A. M. Scudeller, "Nano glass-ceramics from still-making slags," *Quim. Nova*, **25**, 731 – 735 (2002).
8. G. H. Beall and L. R. Pinckney, "Nanophase glass-ceramics," *J. Am. Ceram. Soc.*, **82**, 5 – 16 (1999).
9. L. R. Pinckney and G. H. Beall, "Nanocrystalline nonalkali glass-ceramics," *J. Non-Cryst. Solids*, **219**, 219 – 227 (1997).
10. I. A. Severenkov, E. V. Ustyugova, L. A. Alekseeva, et al., "Glass formation and crystallization of glasses of the strontium aluminosilicate system: influence of modifying additives on melting and crystallization properties," *Glass Ceram.*, **78**(7 – 8), 259 – 263 (2021).
11. L. S. A. Gallo, O. C. Mariana Villas Boas, C. M. Ana, Rodrigues, et al., "Transparent glass-ceramics for ballistic protection: materials and challenges," *J. Mater. Res. Technol.*, **8**, 3357 – 3372 (2019).
12. A. S. Chainikova, M. V. Voropaeva, L. A. Alekseeva, et al., "Current state of developments in the field of radiotransparent cordierite glass-ceramics," *Aviation Mater. Technol.*, No. 6, 45 – 51 (2014). DOI: 10.18577/2071-9140-2014-0-s6-45-51
13. R. D. Rawlings, J. P. Wu, and A. R. Boccaccini, "Glass-ceramics: their production from wastes — a review," *J. Mater. Sci.*, **41**, 733 – 761 (2006).
14. N. Burriesci, C. Arcoraci, P. L. Antonucci, and G. Polizzotti, "Physico-chemical characterization of perlite of various origins," *Mater. Lett.*, **3**, 103 – 110 (1985). DOI: 10.1016/0167-577X(85)90008-4
15. *Aragats Perlite since 1961*. URL: <http://aragatsperlite.am/rus/50/Спецификация>
16. Y. Yu, X. Hao, L. Song, Zh. Li, and Song Li., "Synthesis and characterization of single phase Co-fired cordierite glass-ceramics from perlite," *J. Non-Cryst. Solids*, **448**, 36 – 42 (2016). URL: <http://dx.doi.org/10.1016/j.jnoncrysol.2016.06.039>
17. S. Mercier, A. Molinari, and Y. Estrin, "Grain Size dependence of strength of nanocrystalline materials as exemplified by copper: an elastic-visco-plastic modeling approach," *J. Mater. Sci.*, **42**, 1455 – 1465 (2007). DOI: 10.1007/s10853-006-0670-y
18. T. Kokubo, H.-M. Kim, M. Kawashita, and T. Nakamura, "Novel ceramics for biomedical applications," *J. Austral. Ceram. Soc.*, **36**, 37 – 46 (2000).
19. I. N. Borodin and A. E. Mayer, "Yield limit of nanocrystalline metals under high-speed plastic deformation," *Fiz. Tverd. Tela*, **54**(4), 759 – 766 (2012).
20. A. P. Garshin, V. I. Kulik, and A. S. Nilov, "Impact-resistant materials based on technical ceramics: achievements and prospects for increasing their ballistic efficiency," *Novye Otkrytiya*, No. 4, 53 – 67 (2016).
21. I. Yu. Kelina, L. A. Chevykalova, I. L. Mikhalechik, et al. "Increasing the ballistic efficiency of corundum ceramics," in: *Abstracts. Reports of the 20th International Scientific-Technical Conf. on Designs and Technologies for Producing Products from Non-Metallic Materials* [in Russian], Obninsk (2013), pp. 327 – 329.
22. A. I. Bespalov, V. A. Grigoryan, and I. F. Kobylkin, "Experimental determination of the delay time of penetration of high-speed strikers into ceramic armor," *Defense Technology. Ser. 16. Technical Means of Countering Terrorism*, No. 3 – 4, 84 – 88 (2011).
23. I. N. Frantsevich, F. F. Voronov, and S. A. Bakuta, *Elastic Constants and Elastic Moduli of Metals and Nonmetals* [in Russian], Naukova Dumka, Kiev (1982).
24. A. Benhammou, Y. El Hafiane, and L. Nibou, et al., "Mechanical behavior and ultrasonic non-distractive characterization of elastic properties of cordierite-based ceramics," *Ceram. Int.*, **39**, 21 – 27 (2013).